Direct Imaging of Thermally Driven Domain Wall Motion in Magnetic Insulators

Wanjun Jiang,[1] Pramey Upadhyaya,[1] Yabin Fan,[1] Jing Zhao,[1] Minsheng Wang,[1] Li-Te Chang,[1] Murong Lang,[1] Kin L. Wong,[1] Mark Lewis,[1] Yen-Ting Lin,[1] Jianshi Tang,[1] Sergiy Cherepov,[1] Xuezhi Zhou,[2] Yaroslav Tserkovnyak,[3] Robert N. Schwartz,[1] and Kang L. Wang[1,*]

[1]*Department of Electrical Engineering, Device Research Laboratory, University of California, Los Angeles, California 90095, USA*
[2]*Department of Physics and Astronomy, University of Manitoba, Winnipeg, Manitoba, Canada R3T 2N2*
[3]*Department of Physics and Astronomy, University of California, Los Angeles, California 90095, USA*

(Received 25 July 2012; published 22 April 2013)

Thermally induced domain wall motion in a magnetic insulator was observed using spatiotemporally resolved polar magneto-optical Kerr effect microscopy. The following results were found: (i) the domain wall moves towards hot regime; (ii) a threshold temperature gradient (5 K/mm), i.e., a minimal temperature gradient required to induce domain wall motion; (iii) a finite domain wall velocity outside of the region with a temperature gradient, slowly decreasing as a function of distance, which is interpreted to result from the penetration of a magnonic current into the constant temperature region; and (iv) a linear dependence of the average domain wall velocity on temperature gradient, beyond a threshold thermal bias. Our observations can be qualitatively explained using a magnonic spin transfer torque mechanism, which suggests the utility of magnonic spin transfer torque for controlling magnetization dynamics.

DOI: 10.1103/PhysRevLett.110.177202 PACS numbers: 75.30.Ds, 75.50.Gg, 75.70.Kw, 75.78.Fg

The spin Seebeck effect (SSE) [1,2], has emerged as a novel recipe for generating a room-temperature spin current in the presence of a temperature gradient in various (metallic or insulating) ferromagnets and ferrimagnets; thus, it has attracted a tremendous amount of interest due to its potential to advance spintronics [1–16]. Moreover, it may provide an alternative, perhaps more practical solution for harvesting the heat dissipated in electronic circuits [17]. In magnetic insulators, the SSE is believed to be driven by a magnon distribution that is locally out of equilibrium with its solid-state environment. In addition to magnons (spin waves) [18], domain walls (DWs) are also natural objects existing in ferromagnets [19]. One natural question thus arises: can DWs be experimentally manipulated in magnetic insulators by magnonic currents induced by temperature gradients? This is important, not only for DW based information processing, DW logics, and memories [20,21], but also for validating the magnonic nature of the SSE in magnetic insulators which in part motivates the current study [5,15]. In this Letter, by employing space (360 nm) and time (20 ms) resolved polar magneto-optical Kerr effect (MOKE) microscopy, we present experimental evidence in support of DW motion due to thermally excited magnons in insulating ferrimagnetic yttrium iron garnet (YIG) films.

A temperature gradient can drive DW motion in a magnetic insulator by a mechanism that is analogous to the conduction electron spin transfer torque (STT) mechanism in transition metal ferromagnets [22,23]. Here, the thermally excited magnonic current J_m [5] transfers its spin angular momentum to the local magnetization inside the DW, which in turn yields a spin-wave or magnonic STT [24–26]. Specifically, a total change of spin angular momentum of $2\hbar$ would be imparted by the propagating spin wave to the DW in the absence of angular momentum losses [24–28]. In addition, through observing the amplification of spin wave excitation in the presence of a temperature gradient, Padrón-Hernández *et al.*, have suggested that the local magnetization can be affected by magnonic STT [29], which is also suggested by the observations of the effect of temperature gradient on the ferromagnetic resonance [30].

One key feature of DW motion induced by magnonic STT is that, as a result of the continuity of spin angular momentum, the DW travels in a direction opposite to the direction of spin wave propagation, viz., from the cold region towards the hot region in the presence of a temperature gradient, as predicted theoretically [15,24–28]. The underlying adiabatic approximation is validated as the wavelength of the thermally excited magnons ($\lambda \sim 6$ nm) is smaller than the DW width [$(\sigma_{\mathrm{DW}} \sim \sqrt{A/K_U} \sim 60$ nm): $\lambda/\sigma_{\mathrm{DW}} \sim 0.1$, A is the spin-wave stiffness, and K_U is the effective anisotropy constant] [31]. It is also conceivable that thermal phonon fluxes could contribute to DW motion in magnetic insulators, particularly due to a force exerted on a DW that is thinner than the thermal phonon wavelength. In the opposite, adiabatic limit, magnonic STT is a more natural scenario. This is confirmed by our data, in which DWs move opposite to the direction of the applied heat current.

DW dynamics in YIG in the presence of small temperature gradients can be described by substituting the Walker ansatz into the Landau-Lifshitz-Gilbert equation: $M_s(1 - \alpha\hat{\boldsymbol{m}}) \times \partial_t\hat{\boldsymbol{m}} + \gamma\hat{\boldsymbol{m}} \times H_{\mathrm{eff}} = \gamma\hbar J_m(\partial_x\hat{\boldsymbol{m}} - \beta\hat{\boldsymbol{m}} \times \partial_x\hat{\boldsymbol{m}})$ with the effective magnetic field $\boldsymbol{H}_{\mathrm{eff}} = (K_U m_z)\hat{\boldsymbol{z}} - (2\pi M_s{}^2 m_x)\hat{\boldsymbol{x}} + A\nabla^2\hat{\boldsymbol{m}}$ [24], and magnetization direction

is given by $\hat{\boldsymbol{m}} = (m_x, m_y, m_z)$, M_s is the saturation magnetization, γ is the gyromagnetic ratio, α and β are dimensionless damping constants (as discussed in the Supplemental Material [32]). Below the Walker breakdown, the DW velocity ($v = \partial_t X$) which is quite similar to the current driven DW motion [33], can be written as:

$$v = -\frac{\beta}{\alpha}\frac{\gamma\hbar}{M_s}J_m. \quad (1)$$

For a given temperature gradient (∇T), the magnitude of magnon particle number flux in the x direction, J_m can be estimated as $J_m = -(k_B \nabla T/6\pi^2\lambda\hbar\alpha)\,F_0$, where $F_0 \approx 1$ is a coefficient arising in the kinetic theory of magnonic STT [24,34]. At room temperature (RT), the resultant DW velocity in YIG films in the presence of a temperature gradient $\nabla T = 20$ K/mm can thus be estimated to be $v = 1300\ \mu m/s$ (assuming $\alpha = \beta$) [24]. It should be noted that magnon-magnon, phonon, or disorder scatterings would decreases the DW velocity.

The magnetic systems employed here are 2 μm thick YIG films with a perpendicular anisotropy of composition $(YSmLuCa)_3(FeGe)_5O_{12}$, grown by a liquid phase epitaxial technique on (111) orientated $Gd_3Ga_5O_{12}$ garnet substrates [31]. DW dynamics were monitored using a polar MOKE microscope [19]. The damping factor was estimated to be $\alpha = 0.0075$ based on ferromagnetic resonance, as discussed in the Supplemental Material [32]. Temperature gradients (∇T) were generated by a Peltier Cooler, as confirmed by real time monitoring of the resistances of Pt stripes (width 10 μm, thickness 15 nm). Good thermal contact was made by using silver epoxy. It is noted that the temperature gradient produced by the on-chip Joule heating *should* not be used in YIG films to avoid complications as follows: (a) a magnetic field gradient [31]; (b) spin waves excited by the spin Hall effect (Pt, Ta in particular) [18]; and (c) an inhomogeneous temperature gradient [7,35,36].

Figure 1(a) is a schematic illustration of the experimental setup. Temperature gradients of various magnitudes (∇T) were applied along the x direction, as depicted. During the experiments, the sample is initially saturated ($H = 300$ Oe) and then the field decreased to a constant value ($H = 60$ Oe) that is applied normal to the sample plane in the z direction. In addition, a small in-plane magnetic field (2 Oe) was applied to ensure the regular

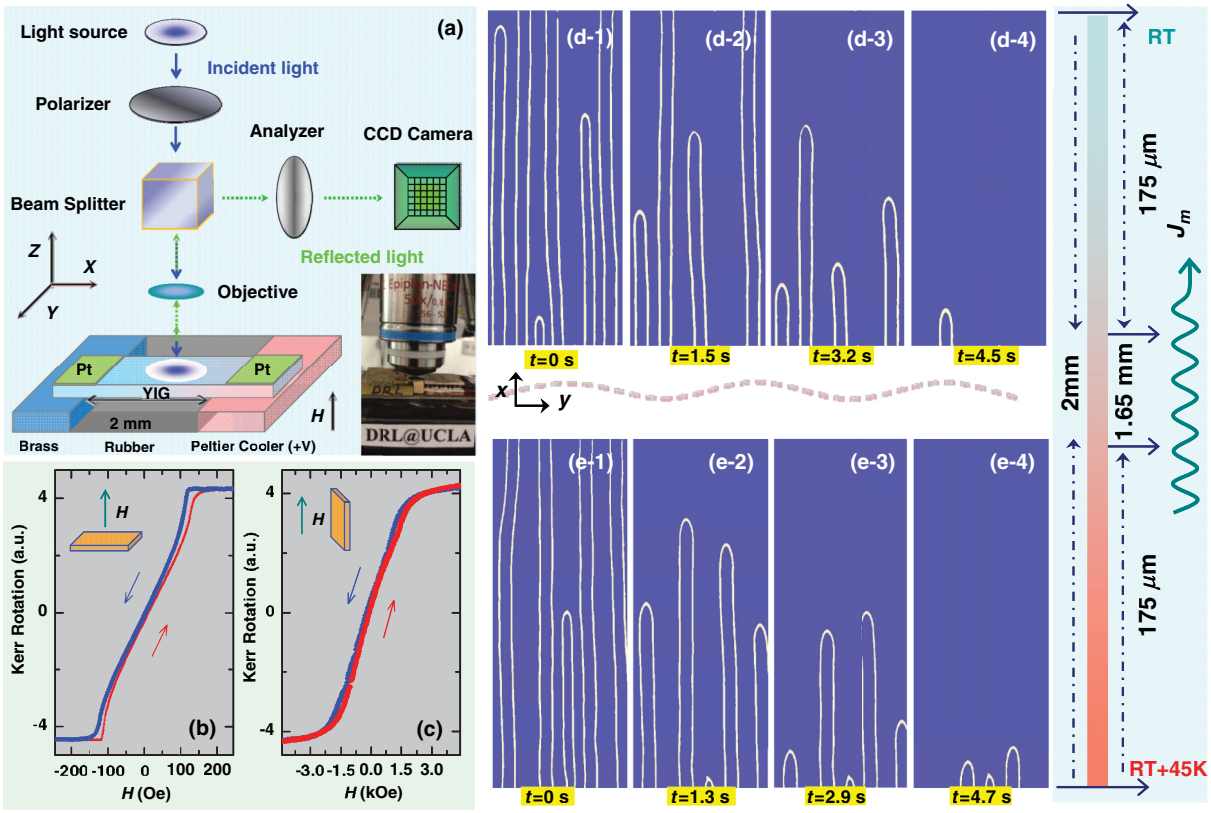

FIG. 1 (color online). Experimental demonstration of DW motion driven by a temperature gradient. (a) The schematic illustration of polar MOKE microscope for DW imaging. (b) and (c) M vs H hysteresis loops measured using a MOKE magnetometer for polar and longitudinal orientations, respectively. (d) Snapshots of the position of the DW as a function of time in the cold region, and hot region (e), respectively. It is noted that there is no time correlation between figures (d) and (e). The blue color corresponds to magnetization along $+z$ direction, and white color associates with the magnetization along $-z$ direction. Each fingerlike pattern thus contains two parallel DWs. These sequential images demonstrate that the direction of motion of the DWs in both cold and hot regions is the same, viz., from the cold region (RT) to the hot region (RT + 45 K), with an average DW velocity of $\bar{v} = 200 \pm 5\ \mu$m/s.

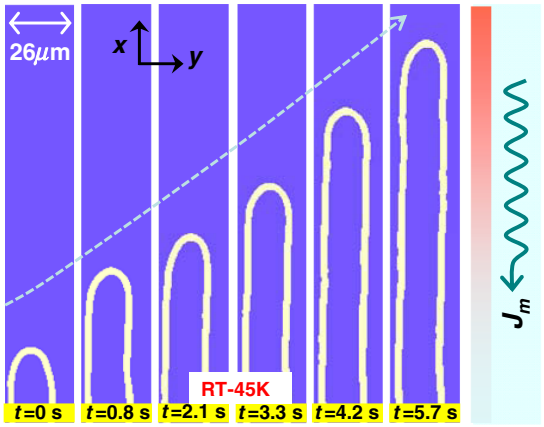

FIG. 2 (color online). Dependence of DW motion on the negative direction of the temperature gradient. Applying the same positive bias magnetic field ($H = +60$ Oe) as used in Fig. 1, with the temperature gradient orientation reversed (viz., $\nabla T = -22.5$ K/mm); again, the direction of motion is preserved, i.e., from the cold end towards the hot end, with an average DW velocity of $\bar{v} = 185 \pm 5$ μm/s.

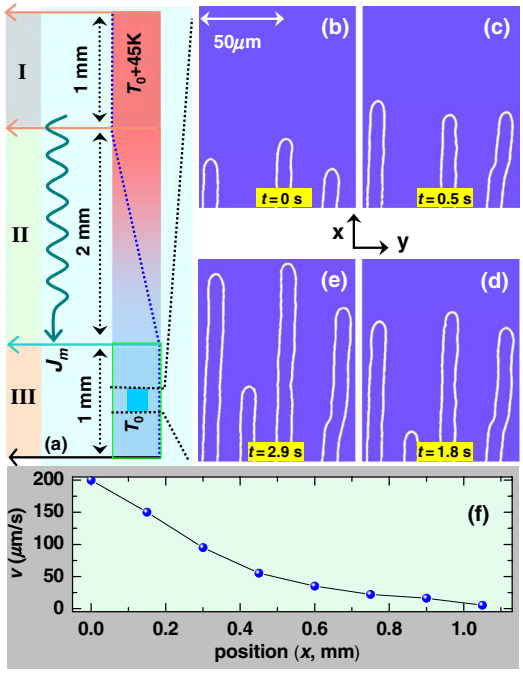

FIG. 3 (color online). Observation of DW motion outside of the region with a temperature gradient. (a) Schematic demonstration of DW motion due to the decaying magnonic current in region (III) of constant temperature (RT), which is away from region (II) with a temperature gradient. Specifically, in region III, $\sim$0.4 mm away from region II with a constant temperature gradient $\nabla T = 22.5$ K/mm, the DW motion is found with an average velocity of $\bar{v} = 90 \pm 5$ μm/s, as shown in Figs. 3(b)–3(e). The reduction in the DW velocity as a function of distance to region II is shown in (f), which can be fitted as $v = v_0 e^{-L/L_0}$ with the characteristic decay length of $L_0 \approx 1$ mm.

domain structures. The above geometry is kept throughout this Letter. Figures 1(b) and 1(c) display MOKE hysteresis loops measured with the magnetic field perpendicular and parallel to the plane of the YIG film, which confirm that the easy axis is normal to the film plane [31]. These data reveal that the out-of-plane saturation field is approximately 135 Oe, whereas the in-plane saturation field is $\sim$1750 Oe; the saturation magnetization $M_s = 84$ emu/cm^3, and $K_U = 610$ J/m^3 was determined using a SQUID magnetometer (see the Supplemental Material [32]).

A polar MOKE microscope was subsequently used to experimentally visualize the time- resolved DW motion driven by the temperature gradient. Sequential images are shown for the cold side in Figs. 1(d1)–(e4) and for the hot side in Figs. 1(e1)–(e4) in the presence of a temperature gradient ($\nabla T = 22.5$ K/mm). It is evident from the above sequential images, the DW moves from the cold region towards the hot region. These experimental results share qualitative features with the corresponding theoretical prediction based on magnonic STT [24–26,28]; i.e., the DW moves from the cold side towards the hotter region in the presence of a temperature gradient.

An important characteristic of the temperature gradient induced DW motion in the present system is that it behaves discontinuously. Specifically, an avalanchelike behavior (refer to the movie given in the Supplemental Material [32]) is observed that differs from its counterpart produced by either a magnetic field, or an electric current [22,23], as well as the corresponding simulation [26]. The occurrence of this avalanchelike behavior is typically related to the Barkhausen effect [19], viz., a sudden change in the size or orientation of magnetic domains. The physical origin of the above jerky behavior lies in the competition between the driving force generated by the magnonic STT and the pinning force produced by defects or impurities (not considered in the corresponding simulation results [26]). It is noted that the average DW velocity $\bar{v}$ is defined in terms of the total DW displacement [$X(t)$] divided by the time when a Barkhausen avalanche occurs (t_1) (i.e., in the time frame where the motion occurs), rather than the total imaging period (t) in order to minimize the scattering in $\bar{v}$ values due to the Barkhausen effect.

For the temperature gradient $\nabla T = 20$ K/mm, one realizes that the measured DW velocity $\bar{v} \approx 200 \pm 5$ μm/s is smaller than the theoretical estimation given previously ($\bar{v} = 1300$ μm/s) [24]. The above differences between theory and experiment may originate from (a) magnon-magnon, phonon, or disorder momentum scatterings [15,24], and (b) the precise value of the ratio β/α is, furthermore, unknown at present for YIG [24].

When a negative temperature gradient ($\nabla T = -22.5$ K/mm) was applied by reversing the input voltage into the Peltier cooler, the direction of magnon propagation is opposite as compared to the positive ∇T. The direction of the DW motion, however, remains the same, viz., from the cold region towards the hot region, in accordance with theory [24–26], as evident in Fig. 2. By analyzing the DW dynamics depicted in Fig. 2, one finds that the average

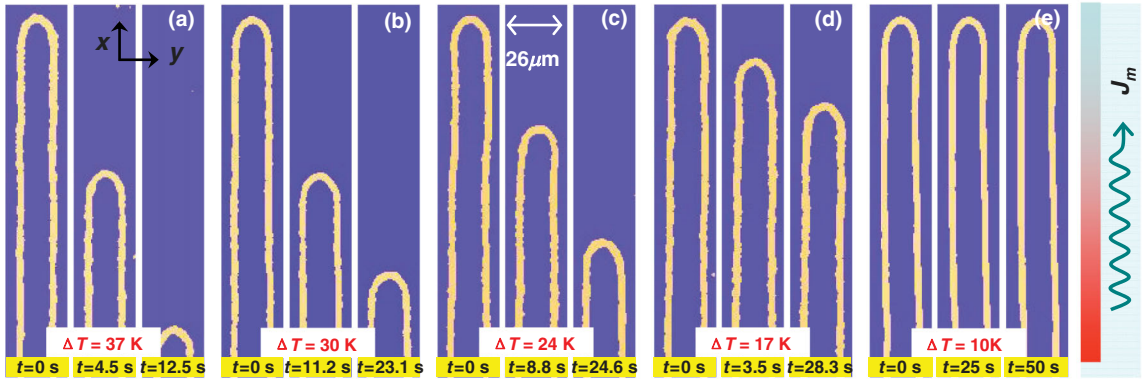

FIG. 4 (color online). Evolutionary demonstration of DW motion under varying temperature gradients. In the presence of the progressively decreasing temperature gradient, one clearly sees that the overall DW displacements decrease and the time intervals spent in traveling increase. These images together yield the decreasing average DW velocity. Here the corresponding temperature gradients for each measurement are (a) $\nabla T = 18.5$, (b) $\nabla T = 15$, (c) $\nabla T = 11.5$, (d) $\nabla T = 8.5$, and (e) $\nabla T = 5$ K/mm.

DW velocity ($\bar{v} = 185 \pm 5$ μm/s) is smaller than the DW motion displayed in Fig. 1. The above observation is consistent with the current driven DW motion in transition metal ferromagnets in which the direction of motion is opposite to the injected current.

As the thermally excited magnons are driven from the hot side towards the cold side, their flux can also penetrate into the cold end that is nominally set at a constant temperature [on top of a thermal bath, which is marked as region III in Fig. 3(a)] [15,37]. Here, in the region of constant temperature, the thermodynamic bias due to the DW energy gradient is consequently minimized [38–41], and the predominant force can be attributed to the magnonic STT that results from the (decaying) magnonic current. Specifically, in region III of Fig. 3(a), ~ 0.4 mm away from region II with a constant temperature gradient $\nabla T = 22.5$ K/mm, the DW motion is found with an average velocity of $\bar{v} = 90 \pm 5$ μm/s, as shown in Figs. 3(b)–3(e). Note that the constant temperature (RT $\pm$ 0.2 K) in this region (III) is confirmed by measuring the resistance of several Pt stripes, shown in the Supplemental Material [32]. Figure 3(f) clearly shows that the measured DW velocity as a function of the distance to region II with a temperature gradient ($\nabla T = 22.5$ K/mm) exhibits an exponential decay. Such a decay function can be empirically fitted by using $v = v_0 e^{-L/L_0}$, where v_0 is the DW velocity in the region with a temperature gradient [marked as II in Fig. 3(a)], v is the DW velocity at varying distance (L) on top of the heat bath; the characteristic length $L_0 \approx 1$ mm is related to the thermalization length of magnons in YIG, which is governed by magnon-phonon and magnon-magnon interactions [15,24]. The same length scale perhaps governs spatial characteristics of the SSE [5]. This experiment also serves as evidence in support of the difference between magnon and phonon thermal distributions, as suggested by other SSE experiments [37]. Our experiment, which is *nonlocal* in nature, can also be extended to metallic systems to avoid the inhomogeneous temperature gradient created by Joule heating [35].

The evolution of DW motion under different temperature gradients was also studied. Selected images are shown in Fig. 4. Clearly, the average DW velocity monotonically decreases as the applied temperature gradient decreases (in the temperature gradient range 5 K/mm $< \nabla T <$ 22.5 K/mm). This behavior is expected as a consequence of the decreasing (average) magnitudes of the excited magnons accompanied with the decreasing applied temperature gradient, which in turn limits the absorbed spin angular momentum. Dependence of $\bar{v}$ vs ∇T is displayed in Fig. 5, which exhibits two distinct features. For 5 K/mm $< \nabla T <$ 22.5 K/mm, an approximately linear function is evident, while for $\nabla T < 5$ K/mm, $\bar{v} = 0$. Specifically, these results reveal the existence of a threshold temperature gradient ∇T_{th} (> 5 K/mm), i.e., a minimal temperature gradient required to overcome the energy barrier, which is analogous to threshold electrical current density J_{th} in current driven DW motion [22,23]. It should be noted that the threshold temperature

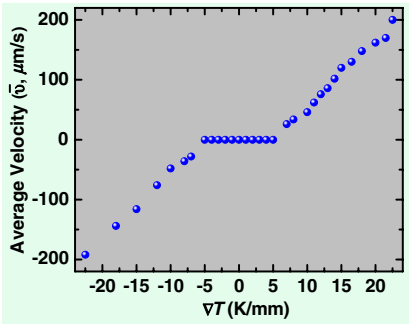

FIG. 5 (color online). Average DW velocity dependence on temperature gradient. The plot of $\bar{v}$ vs ∇T manifests the existence of a threshold temperature gradient $\nabla T_{\text{th}} \approx 5$ K/mm. Here, $\bar{v}$ is an approximately linear function in the temperature range of 5 K/mm $< \nabla T <$ 22.5 K/mm, -22.5 K/mm $< \nabla T < -5$ K/mm, and in the range of -5 K/mm $< \nabla T < 5$ K/mm, $\bar{v}$ is zero.

gradient ∇T_{th} is approximately the same over the 2 mm spacing between the cold and hot sides.

A comparison with electrical current driven DW motion in metallic systems is in order: the threshold current density in metallic systems J_e is typically 10^{11-12} A/m^2, with the accompanied Joule heating resulting in a local temperature increase up to 600–1000 K [22,42]. In contrast, simply by applying a small temperature gradient ($\nabla T > 5$ K/mm) to a magnetic insulator YIG, we have observed pronounced DW motion.

In summary, we have presented the experimental observation of thermally induced DW motion by applying a temperature gradient, which can be qualitatively (as well as semiquantitatively) explained via a magnonic STT. We observed a linear relation of DW velocity with the (positive or negative) temperature gradient, the existence of a threshold temperature gradient, and a decaying magnonic current-induced DW motion in the absence of a temperature gradient in magnetic insulating YIG films. Our results suggest that DWs in insulating magnetic materials can be effectively manipulated by a magnonic STT simply by applying small temperature gradients. Our observations demonstrate that by incorporating a small temperature gradient, insulating magnetic materials could potentially enable thermal spin transfer torque devices [43] in spin caloritronics [2].

Financial support from the Focus Center Research Program-Center on Functional Engineered Nano Architectonics (FENA), the Western Institute of Nanoelectronics (WIN), and the Defense Advanced Research Projects Agency (DARPA) is appreciated. The authors also acknowledge the insightful comments made by Professor Gerrit E. W. Bauer and Dr. Peng Yan. W. J. and P. U. contributed equally to this work.

*wang@ee.ucla.edu; http://drl.ee.ucla.edu/

[1] K. Uchida, S. Takahashi, K. Harii, J. Ieda, W. Koshibae, K. Ando, S. Maekawa, and E. Saitoh, Nature (London) **455**, 778 (2008).
[2] G. E. W. Bauer, E. Saitoh, and B. J. van Wees, Nat. Mater. **11**, 391 (2012).
[3] C. M. Jaworski, R. C. Myers, E. Johnston-Halperin, and J. P. Heremans, Nature (London) **487**, 210 (2012).
[4] C. M. Jaworski, J. Yang, S. Mack, D. D. Awschalom, J. P. Heremans, and R. C. Myers, Nat. Mater. **9**, 898 (2010).
[5] K. Uchida *et al.*, Nat. Mater. **9**, 894 (2010).
[6] M. Walter *et al.*, Nat. Mater. **10**, 742 (2011).
[7] Z. H. Zhang *et al.*, Phys. Rev. Lett. **109**, 037206 (2012).
[8] J.-C. Le Breton, S. Sharma, H. Saito, S. Yuasa, and R. Jansen, Nature (London) **475**, 82 (2011).
[9] M. V. Costache, G. Bridoux, I. Neumann, and S. O. Valenzuela, Nat. Mater. **11**, 199 (2011).
[10] A. Kirihara, K. Uchida, Y. Kajiwara, M. Ishida, Y. Nakamura, T. Manako, E. Saitoh, and S. Yorozu, Nat. Mater. **11**, 686 (2012).
[11] G. E. W. Bauer, A. H. MacDonald, and S. Maekawa, Solid State Commun. **150**, 459 (2010).
[12] G. E. W. Bauer, S. Bretzel, A. Brataas, and Y. Tserkovnyak, Phys. Rev. B **81**, 024427 (2010).
[13] X. Jia, K. Xia, and G. E. W. Bauer, Phys. Rev. Lett. **107**, 176603 (2011).
[14] J. Flipse, F. L. Bakker, A. Slachter, F. K. Dejene, and B. J. van Wees, Nat. Nanotechnol. **7**, 166 (2012).
[15] J. Xiao, G. E. W. Bauer, K. Uchida, E. Saitoh, and S. Maekawa, Phys. Rev. B **81**, 214418 (2010).
[16] J. C. Slonczewski, Phys. Rev. B **82**, 054403 (2010).
[17] F. J. DiSalvo, Science **285**, 703 (1999).
[18] Y. Kajiwara *et al.*, Nature (London) **464**, 262 (2010).
[19] A. Hubert and R. Schafer, *Magnetic Domains: The Analysis of Magnetic Microstructures* (Springer, New York, 2008).
[20] S. S. P. Parkin, M. Hayashi, and L. Thomas, Science **320**, 190 (2008).
[21] D. A. Allwood *et al.*, Science **309**, 1688 (2005).
[22] A. Yamaguchi, T. Ono, S. Nasu, K. Miyake, K. Mibu, and T. Shinjo, Phys. Rev. Lett. **92**, 077205 (2004).
[23] C. H. Marrows, Adv. Phys. **54**, 585 (2005).
[24] A. A. Kovalev and Y. Tserkovnyak, Europhys. Lett. **97**, 67002 (2012).
[25] P. Yan, X. S. Wang, and X. R. Wang, Phys. Rev. Lett. **107**, 177207 (2011).
[26] D. Hinzke and U. Nowak, Phys. Rev. Lett. **107**, 027205 (2011).
[27] P. Yan and G. E. W. Bauer, Phys. Rev. Lett. **109**, 087202 (2012).
[28] X. S. Wang, P. Yan, Y. H. Shen, G. E. W. Bauer, and X. R. Wang, Phys. Rev. Lett. **109**, 167209 (2012).
[29] E. Padrón-Hernández, A. Azevedo, and S. M. Rezende, Phys. Rev. Lett. **107**, 197203 (2011).
[30] L. Lu, Y. Sun, M. Jantz, and M. Wu, Phys. Rev. Lett. **108**, 257202 (2012).
[31] A. P. Malozemoff and J. C. Slonczewski, *Magnetic Domain Walls in Bubble Materials* (Academic, New York, 1979).
[32] See Supplemental Material at http://link.aps.org/supplemental/10.1103/PhysRevLett.110.177202 for details.
[33] In current driven DW motion, a spin angular momentum of $P\hbar$ is transferred by the conduction electron STT to the DW, giving rise to a DW velocity $v = (\beta/\alpha)(P\gamma\hbar J_e/2eM_S)$, where the spin polarization factor $P \sim 40\%$ in transition metal ferromagnets.
[34] A. A. Kovalev and Y. Tserkovnyak, Phys. Rev. B **80**, 100408 (2009).
[35] J. Torrejon, G. Malinowski, M. Pelloux, R. Weil, A. Thiaville, J. Curiale, D. Lacour, F. Montaigne, and M. Hehn, Phys. Rev. Lett. **109**, 106601 (2012).
[36] H. Fangohr, D. S. Chernyshenko, M. Franchin, T. Fischbacher, and G. Meier, Phys. Rev. B **84**, 054437 (2011).
[37] C. M. Jaworski, J. Yang, S. Mack, D. D. Awschalom, R. C. Myers, and J. P. Heremans, Phys. Rev. Lett. **106**, 186601 (2011).
[38] D. Rugar, J. C. Suits, and C. J. Lin, Appl. Phys. Lett. **52**, 1537 (1988).
[39] S. U. Jen and L. Berger, J. Appl. Phys. **59**, 1285 (1986).
[40] S. U. Jen and L. Berger, J. Appl. Phys. **59**, 1278 (1986).
[41] A. A. Thiele, Bell Syst. Tech. J. **48**, 3287 (1969).
[42] A. Yamaguchi, A. Hirohata, T. Ono, and H. Miyajima, J. Phys. Condens. Matter **24**, 024201 (2012).
[43] H. Yu, S. Granville, D. P. Yu, and J.-Ph. Ansermet, Phys. Rev. Lett. **104**, 146601 (2010).